Magnetic phase diagram and antiferromagnetic resonance in $CuGe_{1-y}Si_yO_3$

1997 J. Phys.: Condens. Matter 9 1331

(http://iopscience.iop.org/0953-8984/9/6/016)

J. Phys.: Condens. Matter **9** (1997) 1331–1338. Printed in the UK PII: S0953-8984(97)76649-9

Magnetic phase diagram and antiferromagnetic resonance in $CuGe_{1-y}Si_yO_3$

H Nojiri†, T Hamamoto†, Z J Wang†, S Mitsudo†, M Motokawa†,
S Kimura‡, H Ohta‡, A Ogiwara§, O Fujita§ and J Akimitsu§

† Institute for Materials Research, Tohoku University, Katahira, Sendai 980-77, Japan
‡ Department of Physics, Faculty of Science, Kobe University, Rokkodai, Kobe 657, Japan
§ Department of Physics, Aoyama-Gakuin University, Setagaya-ku Tokyo 157, Japan

Received 24 July 1996, in final form 12 November 1996

Abstract. Magnetization and ESR measurements have been performed on Si-doped $CuGe_{1-y}Si_yO_3$ ($y = 0.01$ and 0.02) single crystals. The $y = 0.01$ sample shows a spin-Peierls transition at $T_{sP} = 11$ K as well as undoped material and additionally show an antiferromagnetic state below $T_N = 2.8$ K. When an external field is applied to the c-axis below T_N, two magnetization jumps due to the spin-flop and the transition from dimerized spin-Peierls phase to magnetic phase are observed at 0.98 T and 11.5 T, respectively, which means the coexistence of spin-Peierls and antiferromagnetic states. On the other hand, the $y = 0.02$ sample shows only an antiferromagnetic transition at $T_N = 4.8$ K.

Since the discovery of a spin-Peierls transition in $CuGeO_3$ [1], extensive studies have been performed theoretically and experimentally. Among them, the impurity effect is an interesting subject which has been very difficult to investigate in organic spin-Peierls compounds. Effects of substituting a different atom such as Zn, Ni, Mg or Mn for the Cu site and Si for the Ge site have been examined so far and the existence of long-range antiferromagnetic (AF) order has been observed in Zn-, Ni-, Mn- and Si-doped samples [2–9]. In the Si-doped sample, the coexistence of dimerized spin-Peierls and AF states below the Néel temperature T_N is the most interesting point. It was reported by Regnault *et al* [7] that the superlattice peaks related to the lattice dimerization were observed even below T_N where AF Bragg peaks appear. It was also found that there are two kinds of magnetic excitation mode below T_N: AF modes and modes related the spin-Peierls phase (SP phase) with a gap. It was pointed out that the observed spectra can be understood as the superposition of two independent spectra. On the other hand, the magnetic phase diagram for the $y = 0.01$ and 0.007 samples was studied by ultrasonic velocity measurements by Poirier *et al* [8]. They concluded that short-range spin-Peierls correlation competes with AF order without any coexistence of the two phases. It was shown theoretically by Fukuyama *et al* [10] that the coexistence of long-range order of lattice distortions and staggered AF moments in impurity-doped spin-Peierls systems are possible. It is stimulating because these two phases have been considered to be exclusive. It has been under discussion whether this model is realized in Si-doped $CuGeO_3$. Recently, the coexistence of SP and AF phases was also found in another neutron scattering experiment [11]. A clear phase diagram of $CuGe_{1-y}Si_yO_3$ was shown by an elastic neutron scattering experiment. An anomaly corresponding to the spin-Peierls transition temperature

0953-8984/97/061331+08$19.50

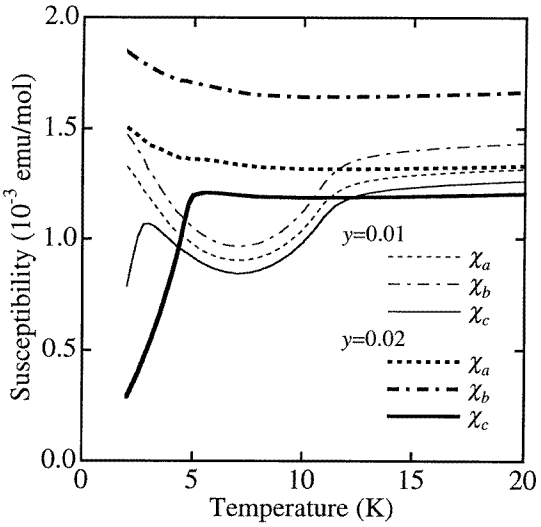

Figure 1. Temperature dependences of the magnetic susceptibilities at 0.5 T. χ_a, χ_b and χ_c are the magnetic susceptibilities when magnetic fields are applied to the a, b and c axes, respectively.

T_{sP} was also found for the $y = 0.01$ sample in heat capacity measurements by Hiroi and co-workers [12]. It was thought desirable perform additional macroscopic and microscopic measurements to study the problem of coexistence in the Si-doped system.

In this paper, we present the results of magnetization measurements up to 30 T to determine the magnetic phase diagrams, especially the phase boundary between the SP phase and magnetic phase (M phase). This phase boundary in Si-doped samples has been determined only by ultrasonic measurements so far [8]. The present results are the first magnetization measurement in high magnetic fields. We also performed ESR experiments to study the nature of magnetic excitations in the Si-doped system. This experiment is also useful to check whether the samples contain two phases. We should be careful in impurity-doped spin systems to exclude the possibility that a sample is composed of different kinds of inhomogeneous macroscopic grains. If a phase separation occurs corresponding to two states, i.e. SP and AF phases exist independently, two different signals corresponding to these two states are expected to be observed. However, if the spin system has a single phase, only one mode will be observed.

$CuGe_{1-y}Si_yO_3$ single crystals with $y = 0.01$ and 0.02 were grown by the travelling-solvent floating-zone method. The starting materials were prepared by mixing CuO (99.9%), GeO_2 (99.99%) and SiO_2 (99.9%). The powder materials were pressed into a rod and sintered at about 1000 °C. The growth rate in the floating-zone process was 1 mm h^{-1} under an O_2 gas flow. The Si concentrations were determined using ICP as 0.99% and 2.05% for the $y = 0.01$ and $y = 0.02$ samples, respectively.

Figure 1 shows the temperature dependences of the magnetic susceptibilities χ_a, χ_b and χ_c below 20 K. The abrupt decreases in χ_c below $T_N = 2.8$ K and 4.8 K for $y = 0.01$ and 0.02 samples, respectively, mean the appearance of AF long-range order. For the $y = 0.01$ sample, the magnetic susceptibility for any of three crystal axes decreases below $T_{sP} = 11$ K, which may be due to the occurrence of the spin-Peierls transition. This agrees with the results of heat capacity measurements [12]. To check the change in the exchange coupling between Cu^{2+} spins by Si doping, magnetic susceptibilities were measured up to

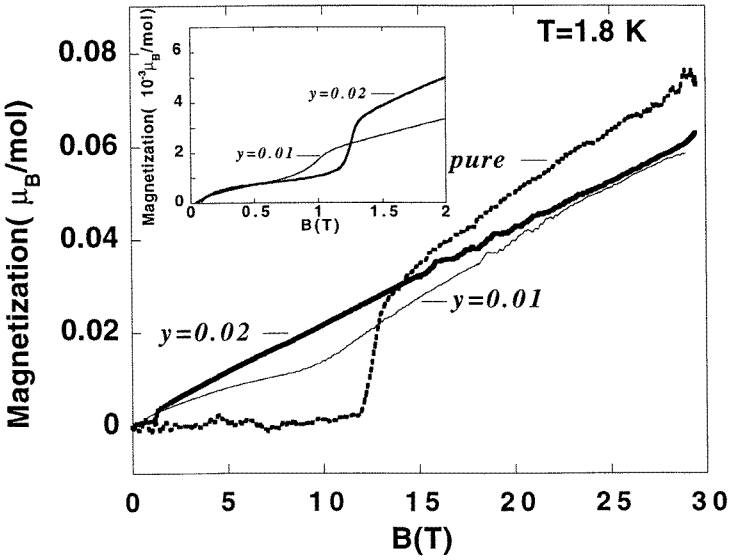

Figure 2. The magnetization curves of the pure (– – –), $y = 0.01$ (——) and $y = 0.02$ (——) samples. Magnetic fields are applied to the c axis. The inset shows the magnetization curves around the spin-flop transition fields for $y = 0.01$ (——) and $y = 0.02$ (——) samples.

180 K for the $y = 0.01$ and the $y = 0.02$ samples. because a magnetic susceptibility changes if the intra-chain exchange coupling is modified. They show quantitative coincidence with that for the pure sample above 20 K.

High-field magnetizations were measured using pulsed fields up to 30 T. When magnetic fields are applied to the c-axis, spin-flop transitions with a small hysteresis were observed below T_N. The transition fields are $H_{SF} = 0.98$ T and 1.29 T for the $y = 0.01$ and 0.02 samples, respectively, at 1.8 K. Magnetization curves up to 30 T are shown in figure 2. For the $y = 0.02$ sample, the magnetization increases linearly to magnetic fields above the spin-flop transition and it reaches $0.065\mu_B$ mol^{-1} at 30 T. There is no nonlinear increase in magnetization corresponding to the transition from the SP phase to the M phase which is observed in pure $CuGeO_3$ at around 12.5 T [13]. On the other hand, the magnetization process of the $y = 0.01$ sample shows a rather broad step at around 11.5 T and the slope of the magnetization curve becomes steeper above this transition. We shall use the notation H_M for the field revealed by this broad step at around 11.5 T in the following. This step is also observed on the a and b axes and the values of the transition fields normalized by the g-values of three crystal axes a, b and c coincide with each other. This behaviour has been reported for pure $CuGeO_3$ [13]. When the temperature increases from 1.8 K, the transition at H_M shows no significant change at around $T_N = 2.8$ K and the step becomes broader and smears out at around 10 K. Figure 3 shows the phase diagram determined by the magnetization measurements using pulsed fields (field scan) and a SQUID magnetometer (temperature scan) for the $y = 0.01$ sample. The results of heat capacity measurements of the same sample [12] are also plotted together. It is unclear whether the phase boundary exists between two regions $H > H_M$, $T < T_N$ and $H > H_M$, $T > T_N$ in our present measurements. No distinct anomaly is observed in heat capacity measurements in magnetic fields above 9 T around T_N. In the following, we explain the phase diagram obtained for the $y = 0.01$ sample before discussing the results of ESR.

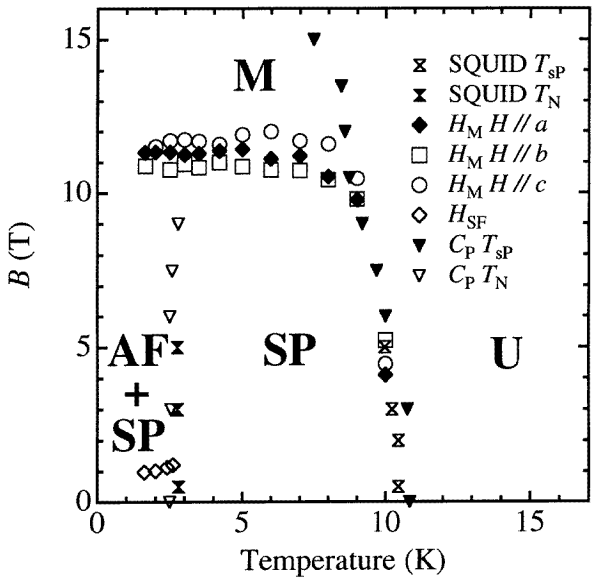

Figure 3. Magnetic phase diagram for the $y = 0.01$ sample. U, SP, AF + SP and M are the uniform (paramagnetic), spin-Peierls, coexisting antiferromagnetic and spin-Peierls, and magnetic phases, respectively. C_p denotes the results of heat capacity measurements [12].

Table 1. The values of α, C_1 and C_2 obtained by fitting the present results with the conventional AFMR modes with orthorhombic symmetry. Values in the Zn-doped case are also shown where the g-values at room temperature are used [9].

	g_a	g_b	g_c	α	C_1 (T^2)	C_2 (T^2)
Pure	2.15	2.25	2.06			
Si (1%)	2.15	2.25	2.06	0.5 ± 0.1	0.39 ± 0.05	0.84 ± 0.1
Si (2%)	2.15	2.25	2.07	0.78 ± 0.06	1.3 ± 0.1	3.8 ± 0.2
Zn (4%) [9]	2.13	2.21	2.01	0.85	0.89	2.1

The existence of a universal phase diagram among different spin-Peierls compounds was pointed out in work on pure $CuGeO_3$ [13]. For the pure system, the SP–M phase boundary has the relation $gH_M^*/2T_{sP}(0) = 1.0$–1.1 T K^{-1} where H_M^* and $T_{sP}(0)$ are the transition field between the SP and M phases and the spin-Peierls transition temperature at zero field, respectively. At the SP–U phase boundary, there is another universal relation expressed as $T_T/T_{sP}(0) \approx 0.8$ where T_T is the temperature at which the SP–U and SP–M phase boundaries merge. For the $y = 0.01$ sample, we obtained $gH_M^*/2T_{sP}(0) \approx 1.1$ and $T_T/T_{sP}(0) \approx 0.78$. So the SP–U and SP–M phase boundaries of the $y = 0.01$ sample can be mapped on to the universal phase diagram as well as other spin-Peierls compounds. As mentioned above, a magnetization step at H_M is observed when below $T_N = 2.8$ K. This shows that the transition at T_N is not a re-entrant transition from the spin-Peierls phase to the normal AF phase. Since a magnetization step at H_M^* or H_M is caused by the collapse of the energy gap by the Zeeman energy in the spin-Peierls system, the observation of a magnetization step at H_M shows the existence of a spin-Peierls gap due to the lattice dimerization. Therefore, below T_N both non-magnetic spin-Peierls states and AF Néel

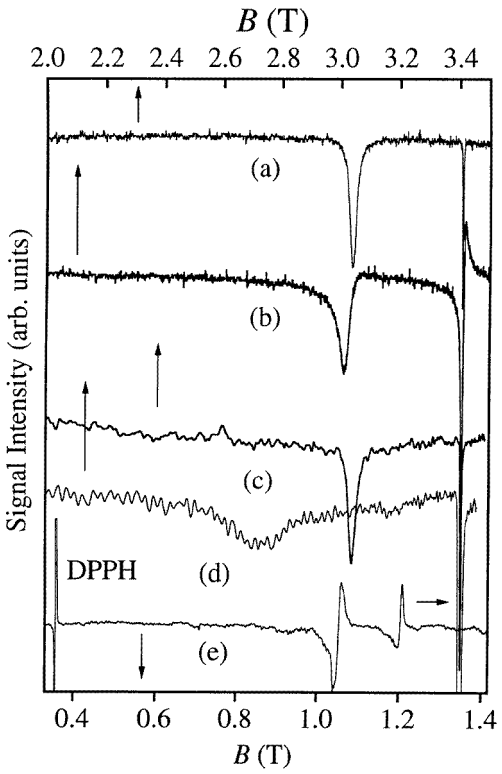

Figure 4. Examples of ESR spectra are shown for (a), (b) $y = 0.01$ and (c), (d) $y = 0.02$ samples. In (a)–(d), magnetic fields are applied to the b axis and the frequency is 95.5 GHz. The sharp resonance at 3.4 T is a signal from DPPH. The temperatures are 30 K for (a) and (c) and 1.7 K and (b) and (d). The spectrum (e) is taken at 1.7 K for the $y = 0.02$ sample at 10 GHz; magnetic fields are applied to the c axis. It was obtained by conventional field modulation methods. The DPPH signal is also shown at a low field.

states coexist with a long-range correlation. This is consistent with the results of neutron scattering experiments in which the superlattice peaks due to the lattice dimerization and AF Bragg peaks are simultaneously observed below T_N [5, 11].

Our present results are somewhat different from the ultrasonic velocity measurements data for the $y = 0.007$ sample obtained by Poirier *et al* [8]. It was reported that the boundary between the AF and SP phases is close to the U–M phase boundary around 9 T. These phase boundaries are different in the present results, as shown in figure 3. In our case, the AF and SP phases coexist below T_N, while it is considered to be a simple AF phase in their results. In spite of the different interpretations, their phase diagram is similar to the present result for the $y = 0.01$ sample. Since $T_{sP}(0)$ in their sample is lower than that of our $y = 0.01$ case, the effective doping concentration in our sample is considered to be lower than that in their sample. This explains the difference between the two phase diagrams.

To obtain the microscopic features of the AF states in the Si-doped sample, we performed ESR experiments. Measurements were made at several frequencies between 10 and 190 GHz with both superconducting and pulsed magnets. Examples of ESR spectra are shown in

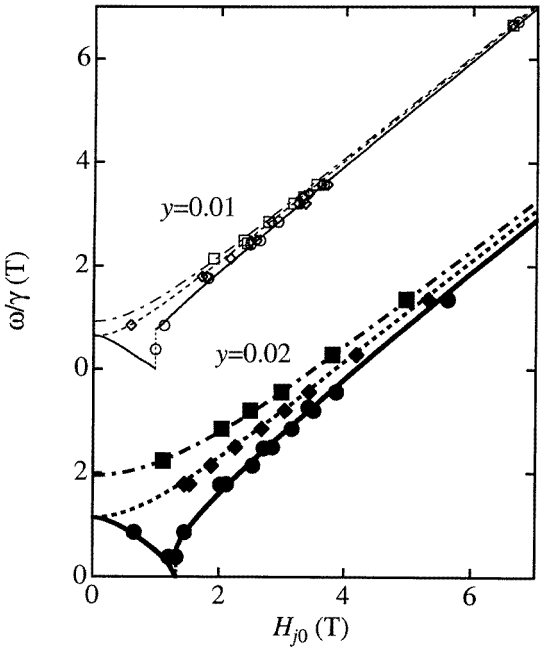

Figure 5. AFMR frequency–field diagrams for the $y = 0.01$ and $y = 0.02$ samples. Magnetic fields are applied to the a (♦, ◇), b (■, □) and c (●, ○) axes. H_{j0} ($j = a$, b and c) are the modified fields normalized by the g-values.

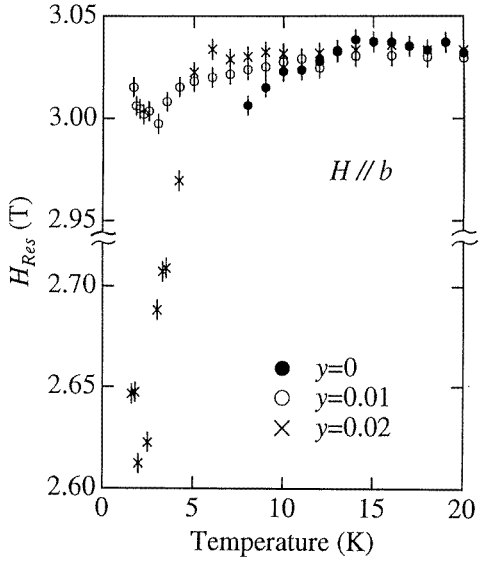

Figure 6. Temperature dependences of the resonance fields H_{Res} at 95.5 GHz for the $y = 0$ (pure), $y = 0.01$ and $y = 0.02$ samples.

figure 4. Figure 5 shows the frequency–field diagram at 1.7 K where $H_{0j} = g_j H/2$ ($j = a$, b, c). The modes show a typical pattern for antiferromagnetic resonance (AFMR) with

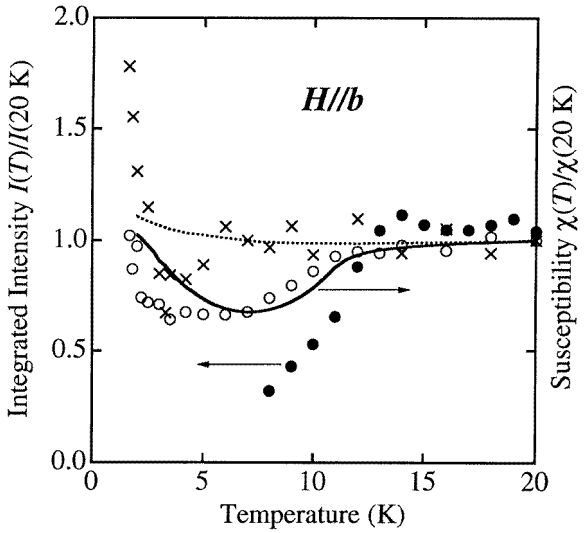

Figure 7. Temperature dependences of ESR intensity at 95.5 GHz for the $y = 0.01$ (○) and $y = 0.02$ (×) samples. The magnetic susceptibilities for H parallel to the b axis are also shown for the $y = 0.01$ (——) and $y = 0.02$ (· · · · · ·) samples. All quantities are normalized at 20 K.

orthorhombic symmetry which was also found by Hase *et al* for a 4% Zn-doped sample [9]. Applying the classical theory for AFMR [14], we obtained the parameters $C_1 = 2AK_1$, $C_2 = 2AK_2$ and $\alpha = 1 - \chi_c/\chi_a$ (χ_c and χ_a are the susceptibilities along the easy and the second easy axes, respectively) as listed in table 1. Here, A and K_i ($i = 1, 2$) are the molecular field coefficient and the anisotropy constants respectively. C_1 is related to spin-flop field H_{SF} as

$$H_{SF} = \sqrt{\frac{C_1}{1 - \chi_c/\chi_a}}. \tag{1}$$

In this procedure, we used the present experimental values of magnetic susceptibilities, H_{SF} and g-value at $T = 60$ K. The directions of easy and hard axes are identical with those of the Zn-doped sample. In the $y = 0.01$ sample, the temperature at which we measured AFMR modes is not sufficiently low compared with $T_N = 2.8$ K and it is necessary to measure these modes in at a much lower temperature to discuss the relation between the Si concentration and the frequencies of the AFMR modes.

Figure 6 shows an example of the shift of the resonance field H_{Res} at 95.5 GHz when the magnetic field is applied to the b axis. For pure $CuGeO_3$, H_{Res} shifts to a lower field below $T_{sP} = 14$ K [15]. In the case of the $y = 0.01$ sample, H_{Res} shows a small shift to a lower field below T_{sP} (= 11 K) and it shows an additional shift when the temperature approaches T_N. In the case of the $y = 0.02$ sample, the shift is observed below 5 K and it shows a large change below T_N for AF ordering. In the whole temperature range of the present measurements, only a single peak is observed.

The temperature dependence of the absorption intensity measured at 95.5 GHz is shown in figure 7. For the $y = 0.01$ sample, it decreases below $T_{sP} = 11$ K as in the case of pure $CuGeO_3$ [15]. In general, it decreases rapidly below T_{sP} where the energy gap opens between non-magnetic singlet and excited triplet states, and the magnetic susceptibility and ESR intensity show similar temperature dependences for the spin-Peierls system.

The behaviour of the ESR signal observed for the $y = 0.01$ sample shows a similarity to that for pure $CuGeO_3$. It is consistent with the results of magnetization measurements which shows that both SP and SF transitions coexist below T_N. Finally we shall discuss the coexistence of phases. For the $y = 0.01$ sample, only a single peak was observed in our ESR experiments. This suggests that dimerized spins and AF ordered spins are coupled and that both contribute to spin-wave excitations below T_N. It is consistent with the theory of Fukuyama *et al* [10] which shows that the magnetic moments are non-zero even in dimerized spins located far from Si impurities. This is considered to be the origin of such coupling and collective excitations such as spin waves in a Si-doped sample.

To summarize, the magnetic phase diagrams are determined in Si-doped $CuGe_{1-y}Si_yO_3$ for the $y = 0.01$ and 0.02 samples by magnetization and magnetic susceptibility measurements. In fields up to 30 T, both the spin-flop transition and the transition from the SP phase to the M phase are observed for $y = 0.01$ samples even below T_N. This suggests the coexistence of long-range order of both SP and AF states below T_N. AFMR modes with orthorhombic symmetry are observed for both concentrations. The ESR signal of the $y = 0.01$ sample shows a single resonance peak in the present measurements which suggests coherence in the coexistence phase between SP and AF ordering.

So that we can discuss quantitatively the relationship between the Si concentration and the magnetic excitations observed in the Si-doped system, ESR measurements in much higher energy and lower temperature ranges are now in progress.

Acknowledgment

This work has been partly supported by a Grant-in-Aid for Scientific Research from the Ministry of Education, Science and Culture.

References

[1] Hase M, Terasaki I and Uchinokura K 1993 *Phys. Rev. Lett.* **70** 3651
[2] Hase M, Terasaki I, Sasago Y and Uchinokura K 1993 *Phys. Rev. Lett.* **71** 4059
[3] Lussier J-G, Coad S M, McMorrow D F and Paul D McK 1995 *J. Phys.: Condens. Matter* **7** L325
[4] Oseroff S B, Cheong S-W, Aktas B, Hundley M F, Fisk Z and Rupp L W Jr 1995 *Phys. Rev. Lett.* **74** 1450
[5] Renard J-P, Le Dang K, Veillet P, Dhalenne G, Revcolevschi A and Regnault L-P 1995 *Europhys. Lett.* **30** 475
[6] Hase M, Sasago Y, Terasaki I, Uchinokura K, Kido G and Hamamoto T 1996 *J. Phys. Soc. Japan* **65** 273
[7] Regnault L P, Renard J-P, Dhalenne G and Revcolevschi A 1995 *Europhys. Lett.* **32** 579
[8] Poirier M, Beaudry R, Castonguay M, Plumer M L, Quirion G, Razavi F S, Revcolevschi A and Dhalenne G 1995 *Phys. Rev.* B **52** R6971
[9] Hase M, Hagiwara M and Katsumata K 1996 *Phys. Rev.* B **54** R3722
[10] Fukuyama H, Tanimoto T and Saito M 1996 *J. Phys. Soc. Japan* **65** 1182
[11] Fujita O, Ogiwara A, Akimitsu J, Katano S, Nishi M, Kakurai K and Fujii Y 1997 to be published
[12] Hiroi M, Hamamoto T, Sera M, Nojiri H, Kobayashi N, Motokawa H, Fujita O, Ogiwara A and Akimitsu J 1997 *Phys. Rev.* B at press
[13] Hase M, Terasaki I, Uchinokura K, Tokunaga M, Miura N and Obara H 1993 *Phys. Rev.* B **48** 9616
[14] Nagamiya T, Yoshida K and Kubo R 1955 *Adv. Phys.* **4** 1
[15] Yamamoto Y, Ohta H, Motokawa M, Fujita O and Akimitsu J 1997 *J. Phys. Soc. Japan* at press